Imaging Cellular Distribution of Bcl Inhibitors Using Small Molecule Drug Conjugates

Randy J. Giedt,[†] Melissa M. Sprachman,[†] Katherine S. Yang,[†] and Ralph Weissleder*[,†,‡]

[†]Center for Systems Biology, Massachusetts General Hospital, 185 Cambridge Street, CPZN 5206, Boston, Massachusetts 02114, United States

[‡]Department of Systems Biology, Harvard Medical School, 200 Longwood Avenue, Boston, Massachusetts 02115, United States

S *Supporting Information*

ABSTRACT: Overexpression of anti-apoptotic proteins such as Bcl-2 is a cellular mechanism to evade apoptosis; consequently, Bcl-2 inhibitors are being developed as anticancer agents. In this work, we have synthesized a fluorescent version of ABT-199 in an effort to visualize a drug surrogate by high resolution imaging. We show that this fluorescent conjugate has comparable Bcl-2 binding efficacy and cell line potency to the parent compound and can be used as an imaging agent in several cancer cell types. We anticipate that this agent will be a valuable tool for studying the single-cell distribution and pharmacokinetics of ABT-199 as well the broader group of BH3-mimetics.
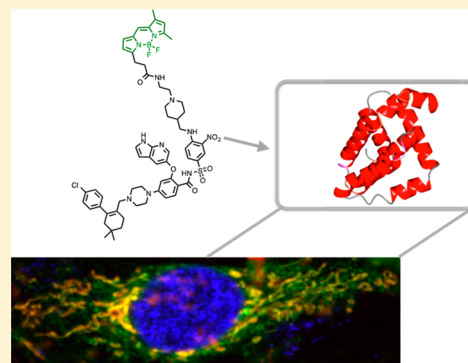
INTRODUCTION

Proteins that regulate cellular apoptotic machinery are critical mediators of cell fate. Overexpression of anti-apoptotic proteins, particularly the B-cell lymphoma 2 (Bcl-2) family of proteins, is one mechanism by which cancer cells evade cell death and become resistant to chemotherapeutic agents. A set of new drug candidates, known as BH3 mimetics, have been developed to target these proteins; several of these candidates are currently undergoing clinical trials. To date, clinical trials have focused mostly on hematopoietic cancers whereas application of these drugs in solid tumors both as single agents and as cotherapeutics is an emerging strategy. Unfortunately, it has not been possible to visualize the distribution of such inhibitors in tumor cells in vivo, making it challenging to determine how effects might vary as a function of tumor type, location, dosing, and other variables. In short, it would be desirable to have a fluorescent companion imaging drug (CID) to explore the spatiotemporal kinetics in vivo.

Bcl-2 plays a fundamental role in cell biology via interactions with a number of other critical proteins, including the pro-apoptotic Bcl-2 family members Bcl-2-associated death promoter (BAD), Bcl-2-antagonist/killer 1 (BAK), Bcl-2 interacting mediator of cell death (BIM), and Bcl-2 associated protein X (BAX).[1−4] Other closely related family members with an anti-apoptotic role exist (Bcl-xL, Bcl2A1, Bcl-w, and Mcl-1), which interact with pro-apoptotic proteins.[4,5] In normal cells, following receipt of a death signal, pro-apoptotic proteins function to permeabilize the outer mitochondrial membrane in order to initiate release of cytochrome c, which combines with apoptosis activating factor (APAF-1) to form apoptosomes, ultimately resulting in apoptosis.[6,7] Anti-apoptotic proteins

inhibit this initiation by a range of interactions with pro-apoptotic proteins. For example, Bcl-2 plays a critical role in this process by preventing cytochrome c release via interactions with BAK/BAX, inhibiting pore formation in the outer mitochondrial membrane.[8,9] The balance of pro- and anti-apoptotic proteins therefore determines overall cell suscepti-bility to normal apoptotic signaling.[10]

Several pan-Bcl-2 family protein inhibitors, including obatoclax (GX15−070),[11] gossypol/levo-gossypol (AT-101),[12] ABT-737,[13] and its orally bioavailable successor Navitoclax (ABT-263) (Figure 1A)[14,15] have been developed; all of these inhibitors have strong interactions with a range of anti-apoptotic proteins. For example, ABT-263 has high affinity for almost all Bcl-2 family anti-apoptotic proteins (K_i <550 nM for Bcl-2, Bcl-xL, Mcl-1, Bcl-w, and Bcl2A1).[5] Despite the initial promise of ABT-263, dose-limiting toxicities were observed from induction of thrombocytopenia, likely due to inhibition of Bcl-xL in platelets.[16] Through rational modification of the ABT-263 scaffold, ABT-199 was developed to selectively target Bcl-2 (Figure 1B).[16,17] This selectivity makes ABT-199 an attractive candidate for development of a CID. The ABT-199 scaffold lends itself to analog generation via a convergent synthetic approach that involves the exchange of a moiety in ABT-199 that is not critical for Bcl-2 affinity. Specifically, the tetrahydropyranyl substituent was exchanged for a piperidine bearing an aminoethyl-linker for conjugation to fluorophores (e.g., BODIPY-FL). We demonstrate that the described CID
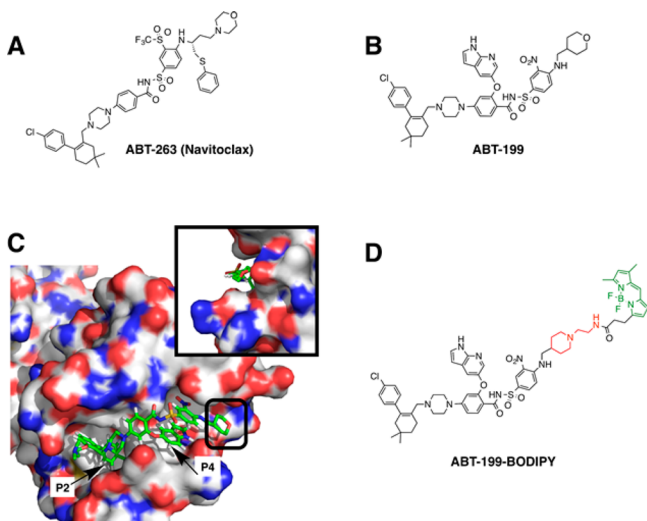
Figure 1. Design of ABT-199-BODIPY. (A,B) Chemical structures of BH3-mimetics ABT-263 (Navitoclax) and ABT-199, (C) Crystal structure of an ABT-199 analog bound to Bcl-2 (PDB 4MAN), generated using The PyMOL Molecular Graphics System, v 1.5.0.4 Schrödinger, LLC. (D) Structure of the fluorescent companion imaging drug (CID) based on the structure of ABT-199.

maintains affinity for Bcl-2 both in vitro and in cellular assays. Furthermore, we show that this agent has high localization to mitochondria (a primary location of Bcl-2 proteins) in cancer cell lines and has shown excellent uptake across a range of tumor lines. Because there is increasing interest in translating ABT-199 into solid tumor therapies in both mono and dual treatment modalities, this CID may be a useful tool for understanding inter- and intracellular localization and heterogeneity of the distribution of Bcl-2 inhibitors.

■ RESULTS

We used both the published crystal structure of Bcl-2 bound to an ABT-199/ABT-263 analog (PDB 4MAN) (Figure 1C) and relevant details related to the BH3-mimetic design to determine available modification sites of ABT-199. From both NMR structural analysis[15] and crystal structure data, it has been established that pro-apoptotic proteins (i.e., BH3 proteins) bind to a groove (approximately 20 Å long), that is composed of two main hydrophobic bonding pockets termed P2 and P4 (Figure 1C).[15,18−20] As described by Souers et al.,[16] the structure of ABT-199 was developed by reverse-engineering of ABT-263 based on slight structural differences in the P4 binding pockets of Bcl-2 and Bcl-xL, namely, the presence of Asp103 in Bcl-2 versus Glu96 in Bcl-xL. Notably, removal of the thiophenolic ether of ABT-263 and incorporation of a 7-azaindole moiety imparted the desired selectivity. The importance of the P2 and P4 binding sites as well as the azaindole moiety in ABT-199 prompted us to modify a portion of the molecule that only occupies the edge of the P4 binding site. We substituted the tetrahydropyranyl moiety of ABT-199 with a piperidine; the piperidine was elaborated with an aminoethyl- linker for facile attachment of fluorophores.

The de novo synthesis (Figure 2) of ABT-199-BODIPY (Figure 1D) was accomplished in 17 steps (11 in the longest linear sequence). The complete synthetic schemes and procedures are provided in the Supporting Information. Starting from known acid **1**, ABT-199 analog **3** was generated after coupling with aryl sulfonamide **2**. Sulfonamide **2** was synthesized via nucleophilic aromatic substitution of commercially available 4-fluoro-3-nitrobenzenesulfonamide with *tert*-butyl 4-(aminomethyl)piperidine-1-carboxylate **6**. Removal of the Boc protecting group with HCl in dioxane followed by alkylation with 1-*N*-(2-bromoethyl)carbamate afforded **2**. Following the EDCI-mediated coupling of **1** and **2** to generate **3**, the Boc protecting group was removed using trifluoroacetic acid (TFA) and Et₃SiH (as a scavenger) followed by reaction
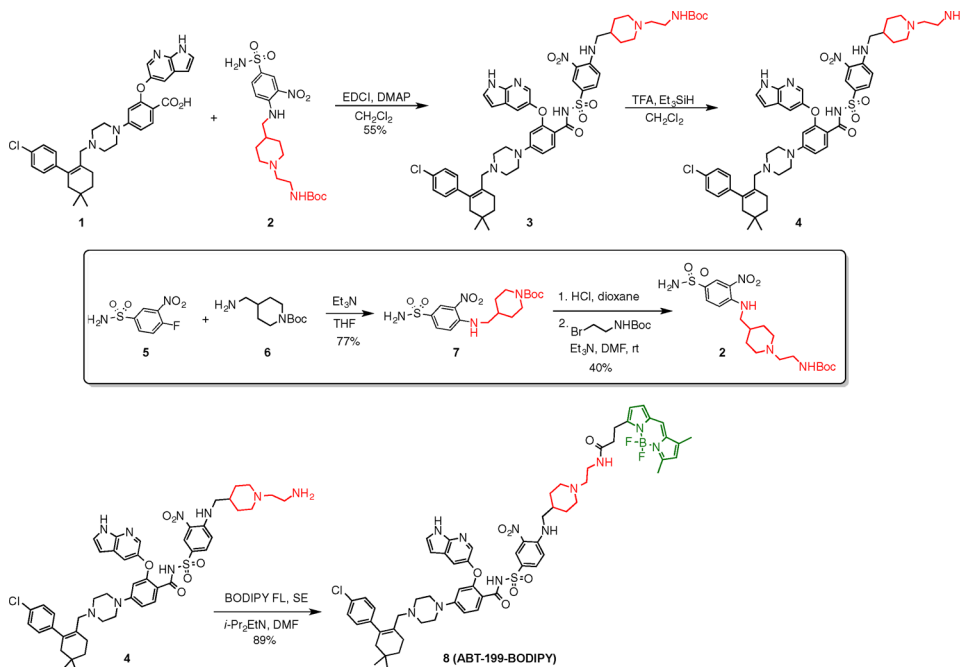

Figure 2. Synthesis of ABT-199-BODIPY.

with the N-hydroxysuccinimidyl ester of BODIPY FL to afford ABT-199-BODIPY **8**. The synthesis of ABT-199-BODIPY is convergent; it would be possible to test other modifications by generating libraries of aryl sulfonamides (accessible in 2−3 steps from commercially available materials) and coupling to intermediate acid **1**. ABT-199-BODIPY was obtained in ca. 9% overall yield over the longest linear sequence. The purity was >95% based on LC-MS analysis (using both evaporative light scattering detection (ELSD) and UV/vis detection for determining purity).

To validate that ABT-199-BODIPY maintains efficacy against Bcl-2, we first performed a competitive binding experiment (Figure 3A). This experiment was carried out by incubating
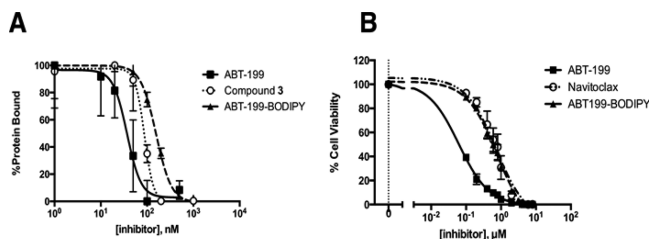
Inhibitor	In vitro activity against isolated Bcl-2 (nM) [95% CI]	Cell viability in an RL cell line IC$_{50}$
ABT-199	36.9 [14.3-95.5]	0.0616 [0.0568-0.0668]
Compound 3	87.7 [66.3-115.9]	ND
ABT-263 (Navitoclax)	ND	0.731 [0.561-0.952]
ABT-199-BODIPY	156.6 [130.7-187.5]	0.767 [0.611-0.963]

Figure 3. Efficacy of ABT-199-BODIPY. (A) Data from an ELISA-based in vitro competitive binding experiment. Varying concentrations of inhibitors were incubated with purified His-tagged Bcl-2 protein (20 nM) for 2 h, then applied to a BIM-coated surface (biotinylated BIM peptide was covalently bound to a Streptavidin-coated plate). The amount of protein bound was quantified after incubation with anti-His_HRP antibody and spectrophotochemical measurement using *ortho*-phenylenediamine as a substrate. (B) Viability of RL cells after incubating with BH3-mimetics for 48 h.

purified Bcl-2 protein with either ABT-199-BODIPY, the piperidine-substituted analog **3**, or ABT-199 (Figure 3A). The binding was assessed using an ELISA-type format wherein the protein/inhibitor complexes were applied to a surface of immobilized BIM peptide.[21] We found that substituting the ABT-199 tetrahydropyran for the N-aminoethylpiperidine (compound **3**) resulted in a 2-fold loss in activity; further elaboration with the BODIPY subsituent resulted in a 4-fold loss of activity; still, the modified ABT-199 scaffolds show excellent inhibitory activity for disruption of the Bcl-2/BIM protein−protein interaction.

We next determined the effects of ABT-199-BODIPY on the viability of RL cells (a human non-Hodgkin's lymphoma derived cell line) which have been shown to have high levels of Bcl-2 and are therefore selectively sensitive to treatment with BH3 mimetics (Figure 3B).[16] ABT-199-BODIPY is ~12 times less effective toward inducing cell death in the RL cell lines, but it is still equipotent with ABT-263, an agent currently in phase II clinical trials. The slight decrease in activity may stem from decreased solubility of ABT-199-BODIPY or reduced affinity of ABT-199-BODIPY due to the addition of the bulkier fluorophore subsituent. ABT-199, ABT-263, and ABT-199-BODIPY were ineffective at inducing cell death in cell lines that

do not overexpress Bcl-2, including OVCA-429 and MDA-MB-231 (EC$_{50}$ > 10 μM, Supporting Information Figure S5).

We next examined the intracellular distribution of ABT-199-BODIPY and its colocalization with apoptosis specific cell components. We first incubated OVCA-429 cells with ABT-199-BODIPY (1 μM, overnight incubation, a concentration shown to be nontoxic to cell lines without specific Bcl-2 dependency; see Supporting Information Figure S5). We observed localization of the imaging drug to mitochondria (Figure 4) as determined by immunocytochemistry. We next
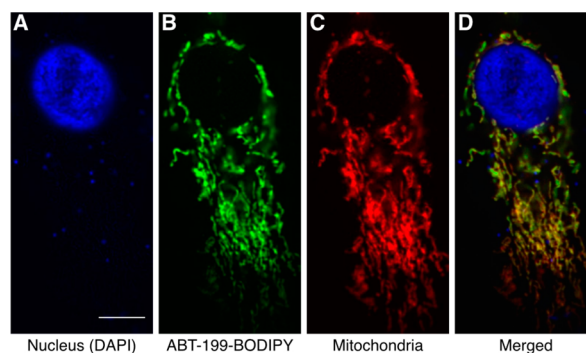

Figure 4. Immunocytochemistry illustrating mitochondrial colocalization of ABT-199-BODIPY in a single OVCA-429 cell. (A) DAPI, (B) ABT-199-BODIPY, (C) TOMM-20 antibody (Mitochondria), (D) Merged imaged (DAPI, blue; ABT-199, green; Mitochondria, red). Scale bar is 5 μm.

imaged the intracellular distribution of ABT-199-BODIPY in live cells. MDA-MB-231 cells transfected with a Bcl-2-RFP reporter were treated with ABT-199-BODIPY (5 μM 1 h before imaging (Figure 5)). In this cell line, Bcl-2 was observed
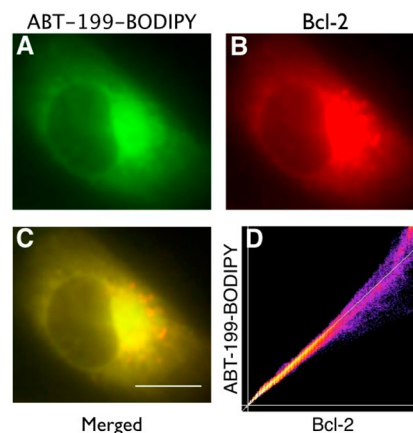

Figure 5. Live cell imaging of ABT-199-BODIPY and Bcl-2 in MDA-MB-231 cells. (A) ABT-199-BODIPY, (B) Bcl-2-RFP, (C) Colocalization of ABT-199-BODIPY (green) and Bcl-2 (red), (D) Colocalization scatter plot of ABT-199-BODIPY and Bcl-2. The Pearson coefficient was 0.9899 and Manders I &II were >0.99. Scale bar is 10 μm.

in the mitochondria in addition to the endoplasmic reticulum and as a cytosolic protein. Addition of ABT-199-BODIPY showed excellent colocalization of the compound with areas of Bcl-2-RFP fusion protein. We similarly assessed whether ABT-199-BODIPY would show similar uptake and localization across a panel of cancer cell lines. Common cell lines (OVCA-429, Panc-1, MDA-MB-231, MCF-7, 4T1, A431, and HT-1080)

were incubated with ABT-199-BODIPY (1 μM) overnight, fixed, counterstained with DAPI, and observed (Figure 6).
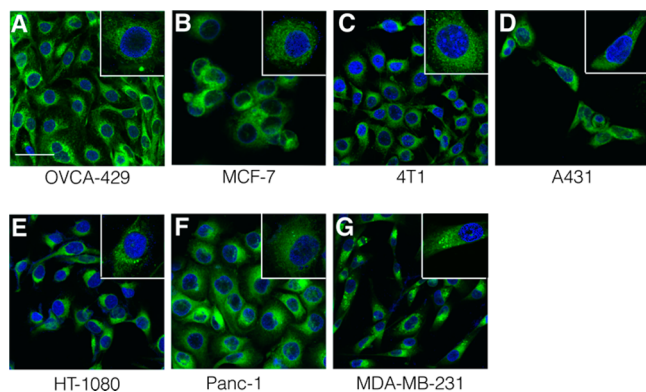

Figure 6. ABT-199-BODIPY localization across a panel of cancer cell lines (DAPI, blue; ABT-199-BODIPY; green). (A) OVCA-429, (B) MCF-7, (C) 4T1, (D) A431, (E) HT-1080, (F) Panc-1, (G) MDA-MB-231. Scale Bar is 50 μm.

Across all cell lines we noted excellent uptake of the CID and colocalization with mitochondria-like structures (Supporting Information Figure S6) in addition to more limited cytosolic and other organelle staining consistent with known localizations of Bcl-2 (Figure 5).

DISCUSSION

The regulation of intrinsic apoptosis events by Bcl-2 family proteins plays a key role in cell fate. Overexpression of Bcl-2 proteins is a common cancer cell survival mechanism. Furthermore, increased expression of Bcl-2 family proteins is a cause of acquired resistance to chemotherapeutic agents. Recently, cancer therapies that target Bcl-2 proteins have shown promise in clinical trials,[22] but little is known regarding the single cell pharmacokinetics, intracellular dynamics, and heterogeneity of distribution of these inhibitors as well as their protein-specific responses.

Current approaches for probing the cellular response of Bcl-2 protein mediated interactions include BH3 profiling, which measures mitochondrial response to BH3-only peptides and is thus predictive of Bcl-2 targeted probes such as ABT-199.[23,24] To understand protein specific dynamics, fluorescence lifetime imaging microscopy (FLIM) using fluorescent proteins (e.g., Venus-Bcl-xL and mCherry-BAD) has also been used to study real-time protein/protein interactions after treatment with inhibitors, but this method does not address the intra- and intercellular distribution of inhibitor.[25,26] To date it has not been possible to directly visualize Bcl-2 inhibitor distribution in live cells.

The increasing interest in targeting Bcl-2 family proteins in nonhematological cancers and solid tumors underscores the need for agents that monitor the distribution and heterogeneity of drug distribution. In this work, we designed and synthesized a structurally matched companion imaging drug (CID) for ABT-199 that can be used as a tool for studying the subcellular localization and pharmacokinetics of Bcl-2 inhibitors. We anticipate that the CID will enable inhibitor localization studies as well as spatiotemporal studies in live cells and tumors. Although we have demonstrated that this CID can be utilized in a range of cancer cells, further testing will be required to move this CID into animal models. The use of such a tool compound

could provide compelling insight toward developing appropriate dual therapy treatment regimens and understanding how cell physiology affects the uptake, localization, and cellular response of BH3-mimetics.

ASSOCIATED CONTENT

Supporting Information

Procedures for chemical synthesis and associated spectra, cell culture and in vitro assays, cell imaging as well as descriptions of all materials and instrumentation. This material is available free of charge via the Internet at http://pubs.acs.org.

AUTHOR INFORMATION

Corresponding Author
*Phone: 617-726-8226. E-mail: rweissleder@mgh.harvard.edu.
Author Contributions
Randy J. Giedt and Melissa M. Sprachman contributed equally to this work.
Notes
The authors declare no competing financial interest.

ABBREVIATIONS

EDCI, 1-ethyl-3-(3-(dimethylamino)propyl)carbodiimide; DMAP, 4-dimethylaminopyridine; TFA, trifluoroacetic acid; THF, tetrahydrofuran; DMF, N,N-dimethylformamide; BODIPY FL, SE, 7-(2-carboxyethyl)-5,5-difluoro-1,3-dimethyl-5H-dipyrrolo[1,2-c:2′,1′-f][1,3,2]diazaborinin-4-ium-5-uide, N-hydroxysuccinimidyl ester; Boc, tert-butyloxycarbonyl

REFERENCES

(1) Murphy, K. M., Ranganathan, V., Farnsworth, M. L., Kavallaris, M., and Lock, R. B. (2000) Bcl-2 inhibits Bax translocation from cytosol to mitochondria during drug-induced apoptosis of human tumor cells. *Cell Death Differ.* 7, 102−111.
(2) Oltvai, Z. N., Milliman, C. L., and Korsmeyer, S. J. (1993) Bcl-2 heterodimerizes in vivo with a conserved homolog, Bax, that accelerates programmed cell death. *Cell* 74, 609−619.
(3) Sedlak, T. W., Oltvai, Z. N., Yang, E., Wang, K., Boise, L. H., Thompson, C. B., and Korsmeyer, S. J. (1995) Multiple Bcl-2 family members demonstrate selective dimerizations with Bax. *Proc. Natl. Acad. Sci. U. S. A.* 92, 7834−7838.
(4) Rual, J. F., Venkatesan, K., Hao, T., Hirozane-Kishikawa, T., Dricot, A., Li, N., Berriz, G. F., Gibbons, F. D., Dreze, M., Ayivi-Guedehoussou, N., Klitgord, N., Simon, C., Boxem, M., Milstein, S., Rosenberg, J., Goldberg, D. S., Zhang, L. V., Wong, S. L., Franklin, G., Li, S., Albala, J. S., Lim, J., Fraughton, C., Llamosas, E., Cevik, S., Bex, C., Lamesch, P., Sikorski, R. S., Vandenhaute, J., Zoghbi, H. Y., Smolyar, A., Bosak, S., Sequerra, R., Doucette-Stamm, L., Cusick, M. E., Hill, D. E., Roth, F. P., and Vidal, M. (2005) Towards a proteome-scale map of the human protein-protein interaction network. *Nature* 437, 1173−1178.
(5) Vogler, M., Dinsdale, D., Dyer, M. J., and Cohen, G. M. (2009) Bcl-2 inhibitors: small molecules with a big impact on cancer therapy. *Cell Death Differ.* 16, 360−367.

(6) Zou, H., Henzel, W. J., Liu, X., Lutschg, A., and Wang, X. (1997) Apaf-1, a human protein homologous to C. elegans CED-4, participates in cytochrome c-dependent activation of caspase-3. *Cell* 90, 405−413.

(7) Milam, S. L., Nicely, N. I., Feeney, B., Mattos, C., and Clark, A. C. (2007) Rapid folding and unfolding of Apaf-1 CARD. *J. Mol. Biol.* 369, 290−304.

(8) Yang, J., Liu, X., Bhalla, K., Kim, C. N., Ibrado, A. M., Cai, J., Peng, T. I., Jones, D. P., and Wang, X. (1997) Prevention of apoptosis by Bcl-2: release of cytochrome c from mitochondria blocked. *Science* 275, 1129−1132.

(9) Komatsu, K., Miyashita, T., Hang, H., Hopkins, K. M., Zheng, W., Cuddeback, S., Yamada, M., Lieberman, H. B., and Wang, H. G. (2000) Human homologue of S. pombe Rad9 interacts with Bcl-2/Bcl-xL and promotes apoptosis. *Nat. Cell Biol.* 2, 1−6.

(10) Youle, R. J., and Strasser, A. (2008) The BCL-2 protein family: opposing activities that mediate cell death. *Nat. Rev. Mol. Cell Biol.* 9, 47−59.

(11) Reed, J. C., and Pellecchia, M. (2005) Apoptosis-based therapies for hematologic malignancies. *Blood* 106, 408−418.

(12) Paulus, A., Chitta, K., Akhtar, S., Personett, D., Miller, K. C., Thompson, K. J., Carr, J., Kumar, S., Roy, V., Ansell, S. M., Mikhael, J. R., Dispenzieri, A., Reeder, C. B., Rivera, C. E., Foran, J., and Chanan-Khan, A. (2014) AT-101 downregulates BCL2 and MCL1 and potentiates the cytotoxic effects of lenalidomide and dexamethasone in preclinical models of multiple myeloma and Waldenstrom macroglobulinaemia. *Br. J. Hamaetol.* 164, 352−365.

(13) Trudel, S., Stewart, A. K., Li, Z., Shu, Y., Liang, S. B., Trieu, Y., Reece, D., Paterson, J., Wang, D., and Wen, X. Y. (2007) The Bcl-2 family protein inhibitor, ABT-737, has substantial antimyeloma activity and shows synergistic effect with dexamethasone and melphalan. *Clin. Cancer Res.* 13, 621−629.

(14) Oltersdorf, T., Elmore, S. W., Shoemaker, A. R., Armstrong, R. C., Augeri, D. J., Belli, B. A., Bruncko, M., Deckwerth, T. L., Dinges, J., Hajduk, P. J., Joseph, M. K., Kitada, S., Korsmeyer, S. J., Kunzer, A. R., Letai, A., Li, C., Mitten, M. J., Nettesheim, D. G., Ng, S., Nimmer, P. M., O'Connor, J. M., Oleksijew, A., Petros, A. M., Reed, J. C., Shen, W., Tahir, S. K., Thompson, C. B., Tomaselli, K. J., Wang, B., Wendt, M. D., Zhang, H., Fesik, S. W., and Rosenberg, S. H. (2005) An inhibitor of Bcl-2 family proteins induces regression of solid tumours. *Nature* 435, 677−681.

(15) Wendt, M. D. (2012) The discovery of Navitoclax, a Bcl-2 family inhibitor. *Top. Med. Chem.* 8, 231−258.

(16) Souers, A. J., Leverson, J. D., Boghaert, E. R., Ackler, S. L., Catron, N. D., Chen, J., Dayton, B. D., Ding, H., Enschede, S. H., Fairbrother, W. J., Huang, D. C., Hymowitz, S. G., Jin, S., Khaw, S. L., Kovar, P. J., Lam, L. T., Lee, J., Maecker, H. L., Marsh, K. C., Mason, K. D., Mitten, M. J., Nimmer, P. M., Oleksijew, A., Park, C. H., Park, C. M., Phillips, D. C., Roberts, A. W., Sampath, D., Seymour, J. F., Smith, M. L., Sullivan, G. M., Tahir, S. K., Tse, C., Wendt, M. D., Xiao, Y., Xue, J. C., Zhang, H., Humerickhouse, R. A., Rosenberg, S. H., and Elmore, S. W. (2013) ABT-199, a potent and selective BcL-2 inhibitor, achieves antitumor activity while sparing platelets. *Nat. Med.* 19, 202−208.

(17) Davids, M. S., and Letai, A. (2013) ABT-199: taking dead aim at Bcl-2. *Cancer Cell* 23, 139−141.

(18) Wendt, M. D., Shen, W., Kunzer, A., McClellan, W. J., Bruncko, M., Oost, T. K., Ding, H., Joseph, M. K., Zhang, H., Nimmer, P. M., Ng, S. C., Shoemaker, A. R., Petros, A. M., Oleksijew, A., Marsh, K., Bauch, J., Oltersdorf, T., Belli, B. A., Martineau, D., Fesik, S. W., Rosenberg, S. H., and Elmore, S. W. (2006) Discovery and structure-activity relationship of antagonists of B-cell lymphoma 2 family proteins with chemopotentiation activity in vitro and in vivo. *J. Med. Chem.* 49, 1165−1181.

(19) Bruncko, M., Oost, T. K., Belli, B. A., Ding, H., Joseph, M. K., Kunzer, A., Martineau, D., McClellan, W. J., Mitten, M., Ng, S. C., Nimmer, P. M., Oltersdorf, T., Park, C. M., Petros, A. M., Shoemaker, A. R., Song, X., Wang, X., Wendt, M. D., Zhang, H., Fesik, S. W., Rosenberg, S. H., and Elmore, S. W. (2007) Studies leading to potent, dual inhibitors of Bcl-2 and Bcl-xL. *J. Med. Chem.* 50, 641−662.

(20) Ni Chonghaile, T., and Letai, A. (2008) Mimicking the BH3 domain to kill cancer cells. *Oncogene* 27 (Suppl 1), S149−S157.

(21) Wang, G., Nikolovska-Coleska, Z., Yang, C. Y., Wang, R., Tang, G., Guo, J., Shangary, S., Qiu, S., Gao, W., Yang, D., Meagher, J., Stuckey, J., Krajewski, K., Jiang, S., Roller, P. P., Abaan, H. O., Tomita, Y., and Wang, S. (2006) Structure-based design of potent small-molecule inhibitors of anti-apoptotic Bcl-2 proteins. *J. Med. Chem.* 49, 6139−6142.

(22) Scarfo, L., and Ghia, P. (2013) Reprogramming cell death: BCL2 family inhibition in hematological malignancies. *Immunol. Lett.* 155, 36−39.

(23) Certo, M., Del Gaizo Moore, V., Nishino, M., Wei, G., Korsmeyer, S., Armstrong, S. A., and Letai, A. (2006) Mitochondria primed by death signals determine cellular addiction to antiapoptotic BCL-2 family members. *Cancer Cell* 9, 351−365.

(24) Vo, T. T., Ryan, J., Carrasco, R., Neuberg, D., Rossi, D. J., Stone, R. M., Deangelo, D. J., Frattini, M. G., and Letai, A. (2012) Relative mitochondrial priming of myeloblasts and normal HSCs determines chemotherapeutic success in AML. *Cell* 151, 344−355.

(25) Kale, J., Liu, Q., Leber, B., and Andrews, D. W. (2012) Shedding light on apoptosis at subcellular membranes. *Cell* 151, 1179−1184.

(26) Aranovich, A., Liu, Q., Collins, T., Geng, F., Leber, B., and Andrews, D. W. (2012) Differences in the mechanisms of proapoptotic BH3 proteins binding to Bcl-XL an d Bcl-2 quantified in live MCF-7 cells. *Mol. Cell* 45, 754−763.

(27) McNicholas, S., Potterton, E., Wilson, K. S., and Noble, M. E. M. (2011) Presenting your structures: the CCP4mg molecular-graphics software. *Acta Crystallogr., Sect. D* 67, 386−94.